

Low-temperature current – voltage characteristics of $\text{YBa}_2\text{Cu}_3\text{O}_{7-\delta}$ films in a magnetic field: direct evidence for a vortex-glass phase*

C. Dekker, W. Eidelloth[†] and R.H. Koch[†]

Faculty of Physics and Astronomy, and Debye Research Institute, University of Utrecht, PO Box 80.000, 3508 TA Utrecht, The Netherlands

[†]IBM Research, T.J. Watson Research Center, PO Box 218, Yorktown Heights, NY 10598, USA

Evidence for a vortex-glass phase is found from nonlinear current–voltage (I – V) characteristics measured on $\text{YBa}_2\text{Cu}_3\text{O}_{7-\delta}$ thin films in high magnetic fields and at low temperatures. Well below the superconducting transition temperature the I – V curves are well described by $E/J = \rho_0 \exp[-(J_0/J)^\mu]$, with E the electric field and J the current density. The exponent μ is 0.19 ± 0.05 for low values of current density and $\mu = 0.94 \pm 0.1$ at high values. The results at low J are characteristic of a vortex glass and constitute the first direct evidence that the low-temperature state of a disordered superconductor is a vortex glass. The results are at variance with predictions from the theory of collective flux creep. Near the phase transition, both ρ_0 and J_0 exhibit critical behaviour.

Keywords: vortex glass; YBCO; magnetotransport

What is the nature of the low-temperature vortex phase in the mixed state of type-II superconductors at intermediate ($H_{c1} < H < H_{c2}$) magnetic fields? In 1957, Abrikosov found that vortex lines of magnetic flux form a periodic vortex lattice with long-range translational order.¹ Larkin, however, showed that the long-range order is destroyed in the presence of random pinning². With the new phenomena encountered in the high T_c superconductors, the answers to the above question have to be reconsidered. New thermodynamic phases have been proposed such as a vortex liquid just below $H_{c2}(T)$ as well as a vortex glass (VG) at lower temperatures^{4,5}. While long-range translational order is absent in both of these phases, the VG phase is predicted to have long-range phase coherence, albeit of a rather complex type^{4,5}. The VG phase is predicted to be truly superconducting in the sense that it has an essentially zero linear resistivity. Note that this is not true for the Abrikosov vortex lattice. Experiments on the nonlinear transport properties of $\text{YBa}_2\text{Cu}_3\text{O}_{7-\delta}$ showed the signatures of a second-order phase transition which was interpreted to occur between the vortex liquid and vortex glass^{5–9}. These experiments, however, did not directly probe whether the low-temperature phase is a vortex glass. Such a direct experimental verification has been absent until now.

Here we present nonlinear transport characteristics of $\text{YBa}_2\text{Cu}_3\text{O}_{7-\delta}$ films at high fields and temperatures down to 5 K, i.e., well below the phase transition. The results verify the predictions from vortex-glass theory, and as such constitute the first direct evidence for the existence of such a phase. The present paper extends our earlier results¹⁰. Over a wide range of fields and temperatures, the functional form of the nonlinear current–voltage (I – V) characteristics is found to be well described by

$$\rho \equiv \frac{E}{J} = \rho_0 \exp \left[- \left(\frac{J_0}{J} \right)^\mu \right] \quad (1)$$

where ρ is the nonlinear resistivity, E is the electric field, J is the current density, and J_0 and ρ_0 are the characteristic current density and resistivity, respectively. The present experiments yield $\mu = 0.19 \pm 0.05$ at low current densities and $\mu = 0.94 \pm 0.1$ for high J . Equation (1) has been proposed for VG theory^{4,5} and our results are consistent with the low-temperature phase being a vortex glass. An alternative theory which yields the form given in Equation (1) is the theory of collective flux creep¹¹. The experimentally deduced current–density dependence of the exponent μ , however, is in contrast to predictions of this theory, both qualitatively and quantitatively.

*Paper presented at the conference 'Critical Currents in High T_c Superconductors', 22–24 April 1992, Vienna, Austria

Experiment

Epitaxial *c*-axis-up YBa₂Cu₃O_{7-δ} films of thickness 300 nm were grown by laser ablation on (100) SrTiO₃. Although several films were investigated, we here present the results for one film only (sample STO2). The films exhibited zero resistance near 90 K and critical current densities (from a 1 μV cm⁻¹ criterion) of about 10¹⁰ A m⁻² at 77 K and 0 T. Photolithography and Ar-ion milling techniques were used to define four-probe patterns with sample areas of typical width 2–4 μm and length 100–200 μm. Au contact pads that were (200 μm)² in area yielded contact resistivities of $\ll 10^{-8} \Omega \text{ m}^2$ after annealing. The *I*-*V* curves are measured with an a.c. method as previously discussed in reference 1: individual current and voltage characteristics were averaged typically 5000 times for each value of temperature. The current-induced heating of the sample, estimated from the increase in temperature of the sample with increased power, was estimated to be much less than 0.5 K. Magnetic fields from 0.02 to 5 T were applied perpendicular to the film, i.e. $\vec{H} \parallel \vec{c}$. Temperatures ranged from above the VG transition temperature (which, for example, equals ≈ 73 K for 5 T) down to 5 K.

Near the VG phase transition at high temperatures, the nonlinear *I*-*V* curves exhibit critical scaling behaviour, as reported before⁶. Here, however, we concentrate on the form of the *I*-*V* curves at low temperatures, i.e. $T \ll T_g$. Figure 1a shows an example of an *I*-*V* curve at 39 K and 1 T on a log-log plot. We attempt a fit of Equation (1) to the data. To find μ, Equation (1) can be recast as an equation for a straight line by taking its logarithm, $\ln \rho = \ln \rho_0 + m \times [-J^{-\mu}]$, where *m*, the slope, is given by J_0^μ . We thus replot the data as $\ln \rho$ vs $-J^{-\mu}$ for different values of μ (see Figure 1b). Conformity of the data to a straight line on such a plot signifies a satisfactory fit of Equation (1) and allows μ to be determined. Indeed, this equation was found to describe the data adequately for all *T*, *B* and *J*. Subsequently, *J*₀ and ρ₀ are directly found from the slope and the ordinate, respectively. The advantage of this procedure is that it replaces the simultaneous fitting of three parameters with substantial mutual correlations by the adjustment of only one parameter, μ.

The temperature dependence of μ is given in Figure 2a. Two plateaux in the value of μ are found: at high temperature μ ≈ 0.19, but, upon lowering temperature, μ gradually increases until ultimately μ ≈ 0.94. The crossover between the two plateaux can also be observed in the magnetic-field dependence of μ, as shown elsewhere¹⁰. The result at various temperatures and fields for this sample may be summarized in Figure 3: at high temperatures and fields we find a regime (which for the present sample is rather narrow) where μ = 0.19 ± 0.05, while at low temperatures and fields μ = 0.94 ± 0.1. In between, a rather broad crossover regime is found. What is the reason for this pronounced temperature dependence of μ? It should be realized that with a change in *T* or *B*, one always has to adjust the current scale in order to observe the dissipation within our fixed voltage window. We have found that it is in fact the current density which controls the value of μ. Figure 2b shows a plot of μ versus *J*. (For this current density we take the average value of the current-density range

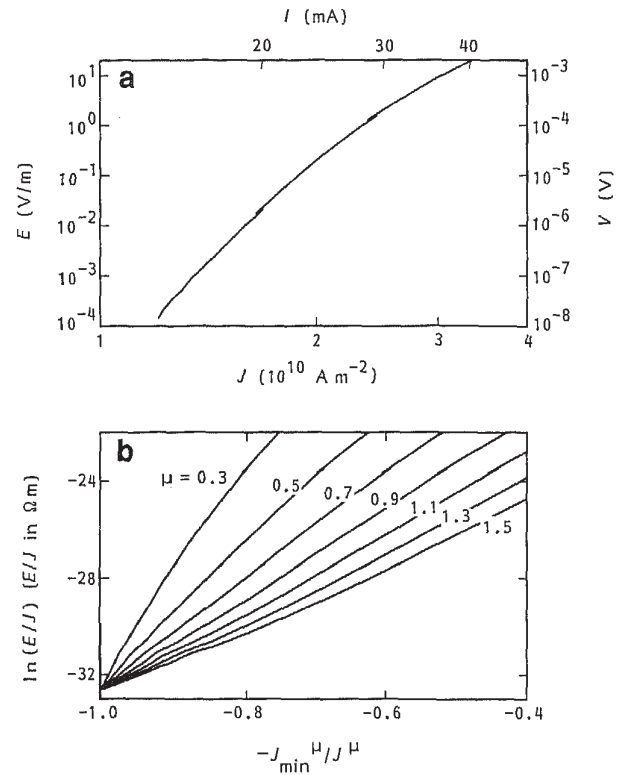


Figure 1 (a) Example of an *I*-*V* curve shown on a log-log plot; $T = 39 \text{ K}$, $B = 1 \text{ T}$, sample STO2. The *I*-*V* curve was measured with three different a.c. current amplitudes. The slight disconnections between the three parts of the *I*-*V* curve result from small ($\sim 0.1 \text{ K}$) heating effects; cf. the discussion in reference 6. (b) Example of the data analysis: plot of $\ln(E/J)$ vs $-J^{-\mu}$ at various μ for the *I*-*V* curve shown in (a). The current densities are normalized to the minimum value J_{min} to allow comparison for different μ in one figure. The experimental data conform to a straight line only near $\mu = 0.9$, but show curvature for the different values

over which Equation (1) fits the data.) The figure contains all of our data for temperatures from 5 to 70 K and fields from 0.02 to 5 T for sample STO2. There is substantial experimental scatter, but the data collapse convincingly shows that μ depends, at least primarily, on *J* rather than on *T* or *B*. Finally, we note that the current dependence of μ has also been checked directly by analysing the *I*-*V* characteristics within a fixed range of current densities. We then find a μ value which, within errors, is constant as a function of field or temperature. For example, for the range $3\text{--}6 \times 10^9 \text{ A m}^{-2}$ we find $\mu = 0.6 \pm 0.1$ for temperatures from approximately 40 to 60 K.

We now turn to the result for the other two parameters in Equation (1), *J*₀ and ρ₀. Both exhibit quite strong *T* and *B* dependences which can be explained by a crossover between rather different values in the two plateau regimes for μ found earlier. Figure 4, for example, shows *J*₀(*T*). It is seen that *J*₀ first decreases slightly with temperature. Near 30 K, i.e., at the point where μ starts to deviate from its 0.94 plateau, *J*₀ increases sharply, whereas *J*₀ decreases again above ≈ 55 K, i.e., where μ saturates at 0.19. At all temperatures, *J*₀ substantially exceeds the experimental range of *J*, validating the use of Equation (1) for the analysis. For high *T* and μ = 0.19, we find that *J*₀(*T*)

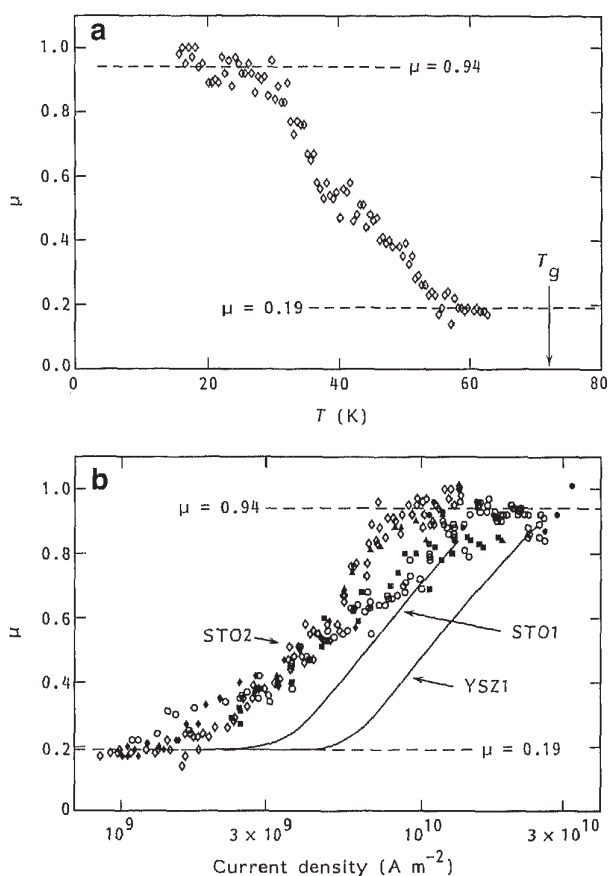


Figure 2 (a) Temperature dependence of μ for $B = 5$ T, sample STO2. The arrow denotes the vortex-glass transition temperature T_g . (b) μ vs the current density for STO2. (For this current density we take the average value of the current-density range over which Equation (1) fits the data.) Symbols represent data from I - V curves at various T and B . The data collapse indicates that μ depends on J rather than on T or B . Solid lines indicate similar data for two different samples, STO1 and YSZ11

approaches the critical behaviour $J_0 \propto (1 - T/T_g)^{2\nu}$. $\rho_0(T)$ similarly goes as $\rho_0 \propto (1 - T/T_g)^{(z-1)\nu}$. (As is evident from inspection of Figure 2, the statistical error in μ is quite substantial. If μ is not fixed at the average plateau value, the appreciable scatter for J_0 and ρ_0 prohibits the analysis of their detailed T and B dependences.) The resultant exponents $\nu = 1.8 \pm 0.2$ and $z = 6 \pm 2$, which are here extracted from the critical behaviour below T_g , compare excellently with previously reported values, $\nu = 1.7$ and $z = 4.9$, deduced above and at T_g , respectively⁶⁻⁹. For low T and $\mu = 0.94$, we obtain $J_0 \propto 1/T^{1.2 \pm 0.2}$. Such an approximate $1/T$ dependence is anticipated since Equation (1) derives^{4,5,11} from a thermally activated resistivity $\rho \propto \exp(-U/k_B T)$, with an energy barrier $U \propto J^{-\mu}$, and correspondingly, J_0 should be proportional to $1/T^{1/\mu}$.

Discussion

The main experimental result from the present work is the exponent μ which appears to dependent on the current density. One may be surprised that the fit of Equa-

tion (1) to $\rho(J)$ involves a parameter μ which itself also depends on current density. However, we will argue below that there is an underlying physical mechanism why μ should be different for different current densities. In fact, a current-dependent μ was already proposed theoretically by Feigel'man *et al.*¹¹. We shall now give a physical picture which yields a plausible scenario to explain the experimental findings.

Both the VG theory^{4,5} and the most commonly cited alternative explanation, collective flux creep¹¹, lead to Equation (1). The two theories, however, predict different values for μ . Both theories envision dissipation by jumps of segments of vortex bundles ('vortex loops') in a disordered Abrikosov lattice. Yet they approach it from opposite limits. Whereas the VG theory describes the behaviour at long length scales, the collective-creep theory considers shorter length scales, namely, the case where the randomness is weak enough to enable a description of the local vortex lattice in terms of elastic-media theory. The characteristic vortex-loop size l that is probed in an experiment will be larger for smaller applied current densities^{4,5,11}. In other words, measurements at different current densities probe the dynamics of vortex loops of different typical size. The collective-creep theory yields different μ for different regimes of l : μ is predicted to equal $1/7$ for small loops (at high J), $\mu = 3/2$ in an intermediate regime, and $\mu = 7/9$ for the longest length scale¹² considered, i.e., at low J ¹¹. (A similar scaling approach yields $\mu = 1/2$ for large loops^{12,13}.) Note that this trend from small to large μ values with decreasing current density is opposite to that observed in Figure 2b. Moreover, the values quoted for the longest length scales are inconsistent with the present experimental result $\mu = 0.19 \pm 0.05$ at low J , i.e. large l . This small μ value, however, fits the VG picture particularly well since $0 < \mu \ll 1$ is expected, because the three-dimensional VG appears to be only slightly above its lower critical dimensionality¹⁴ where $\mu = 0$. A consistent picture of an equilibrium VG phase thus appears from the present work together with the evidence for the phase transition. Figure 3 summarizes the resulting phase diagram with a low-temperature VG phase and a high-temperature normal (non-superconducting vortex liquid) phase. Note that the equilibrium VG phase will only be probed in the limit of a vanishing current density (i.e., long length scales).

This explains the small μ value at low current density. But what about the increase of μ with J as well as its saturation near 0.94 at high J ? The dynamics of the VG loops will only be probed at low current density, or equivalently, at long length scales. Here, 'long' is defined by the condition that the vortex loop size is larger than any microscopic length scale which locally might disrupt the VG ground-state configuration of vortex positions. In the present case, this length scale is set by the remnant short-range translational order of the vortex lines. For the laser-ablated films, we have found that the translational order is limited to very short distances of a few vortex spacings only¹⁰. Consequently, the VG behaviour is, for the films, perceptible up to relatively high current densities ($\sim 10^9$ - 10^{10} A m⁻²). If one measures the dissipation at even higher current densities, one will probe the dynamics of vortex loops with a size that is of the order of a few vortex spac-

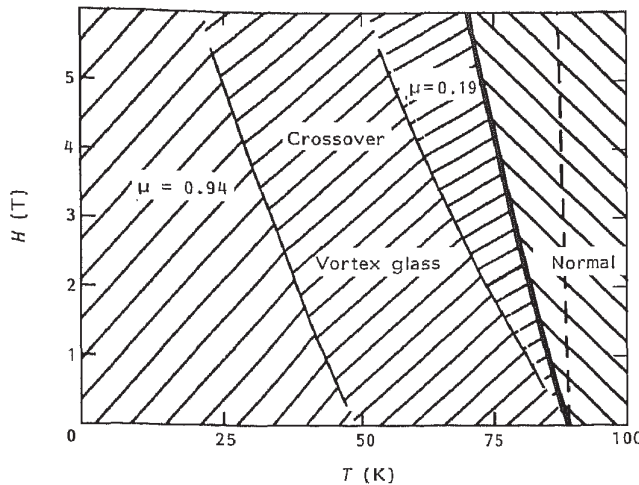


Figure 3 H, T diagram showing the various regimes for μ as found for sample STO2. The thick solid line denotes the vortex-glass phase transition. It should be stressed that the equilibrium phase (probed at vanishing applied current density) at all temperatures below the phase transition is a vortex-glass phase. In other words, one should not identify the various regimes for μ with new vortex phases. Above the phase transition, one has the normal (i.e. non-superconducting) phase. The dashed line represents the mean-field $H_{c2}(T)$

ings or smaller. The different μ value (0.94 ± 0.1) that is observed in the experiment thus signifies that the dynamics in this case are quite different from the VG dynamics. For the present films, which exhibit translational order over a few vortex spacings only, we expect that the relevant vortex loops at high J involve single vortex lines only. For single vortex lines interacting with weakly pinning point defects, μ has been

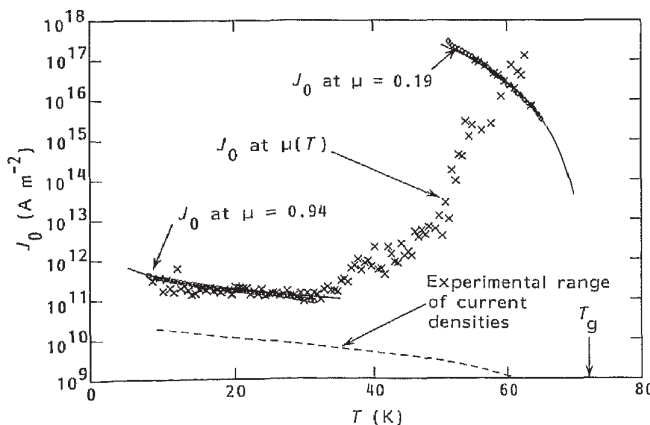


Figure 4 J_0 vs T . Denoted are the results of the fit of Equation (1) (\times) as well as the results from fits where μ was fixed at either 0.94 (\circ) or 0.19 (\diamond). The dashed line represents the typical experimental range of current density where the $I-V$ curves were taken. The arrow denotes the vortex-glass transition temperature T_g . Solid lines represent $J_0 \propto 1/T^{1.2}$ and $J_0 \propto (T_g - T)^{2\nu}$ at low and high temperature, respectively, as discussed in the text

calculated¹¹ to equal 1/7, which clearly is at variance with the experimental $\mu = 0.94 \pm 0.1$. We propose that the major source of pinning in the films instead involves linear or planar defects with some extent along \vec{c} such as stacking faults, micro-twins, dislocations, etc. A simple estimate for $U(J)$ shows that $\mu = 1$ for this case¹⁵, which is in agreement with the experimental result.

More generally, the VG behaviour at long length scales should be universal, whereas the behaviour encountered at high current densities will be non-universal because it will be strongly dependent on the detailed microscopic properties of the material.

Conclusions

The $I-V$ curves are well described by Equation (1), with an exponent μ which is current-dependent. Whereas the results at low current density provide direct evidence for a vortex-glass phase, the findings at high current density signal the non-universal behaviour at very short length scales. The crossover between these regimes is controlled by the size of the 'Abrikosov-lattice domains', which in the films amounts to only a few vortex spacings. The results are at variance with predictions from the theory of collective flux creep.

Acknowledgements

We thank Matthew P.A. Fisher as well as V.D. Geschkenbein, T.A. Tokuyasu, J. Toner, and V.M. Vinokur for discussions. We acknowledge the experimental support of W.J. Gallagher, C.D. Jessen, R.B. Laibowitz, A.M. Torressen, R.L. Sandstrom, and P.J.M. Wöltgens. This work was partially supported by the US Office of Naval Research. One of us (C.D.) has been supported by a NATO Science Fellowship and by the Netherlands organization Nederlandse Organisatie voor Zuiver Wetenschappelijk Onderzoek (NWO).

References

- 1 Abrikosov, A.A. *Zh Eksp Teor Fiz* (1957) **32** 1442 [*Sov Phys JETP* (1957) **5** 1174]
- 2 Larkin, A.I. *Zh Eksp Teor Fiz* (1970) **58** 1466 [*Sov Phys JETP* (1970) **31** 784]
- 3 Larkin, I. and Ovchinnikov, Yu.N. *J Low Temp Phys* (1979) **34** 409
- 4 Fisher, M.P.A. *Phys Rev Lett* (1989) **62** 1415
- 5 Fisher, D.S., Fisher, M.P.A. and Huse, D.A. *Phys Rev B* (1991) **43** 130
- 6 Koch, R.H., Foglietti, V., Gallagher, W.J., Koren, G., Gupta, A. and Fisher, M.P.A. *Phys Rev Lett* (1989) **63** 1511
- 7 Gammel, P.L., Schneemeyer, L.F. and Bishop, D.J. *Phys Rev Lett* (1991) **66** 953
- 8 Worthington, T.K., Olsson, E., Nichols, C.S., Shaw, T.M. and Clarke, D.R. *Phys Rev B* (1991) **43** 10539
- 9 Olsson, H.K., Koch, R.H., Eidelloth, W. and Robertazzi, R.P. *Phys Rev Lett* (1991) **66** 2661
- 10 Dekker, C., Eidelloth, W. and Koch, R.H. *Phys Rev Lett* (1992) **68** 3347
- 11 Feigel'man, M.V., Geschkenbein, V.B., Larkin, A.I. and Vinokur, V.M. *Phys Rev Lett* (1989) **63** 2303
- 12 Nattermann, T. *Phys Rev Lett* (1990) **64** 2454
- 13 Fisher, K.H. and Nattermann, T. *Phys Rev B* (1991) **43** 10373
- 14 Reger, J.D., Tokuyasu, T.A., Young, A.P. and Fisher, M.P.A. *Phys Rev B* (1991) **44** 7147
- 15 Fisher, M.P.A. Private communication